Geothermal industry waste-derived catalyst for enhanced biohydrogen production

Siti Munfarida [a], Widayat [a, b, c, *], Hantoro Satriadi [a], Bambang Cahyono [d], Hadiyanto [a, b], John Philia [a, c], Jedy Prameswari [a, c]

[a] Chemical Engineering Department, Faculty of Engineering, Diponegoro University, Semarang, 50275, Indonesia
[b] Center of Biomass and Renewable Energy, Diponegoro University, Semarang, 50275, Indonesia
[c] Advanced Materials Research Laboratory, Diponegoro University, Semarang, 50275, Indonesia
[d] Chemistry Department, Faculty of Mathematics and Science, Diponegoro University, Semarang, 50275, Indonesia

HIGHLIGHTS

- Catalyst showed promising performance in biohydrogen production.
- Si/Al ratio and wash treatment was significant to catalyst yield.
- Si/Al ratio and wash treatment was significant to biohydrogen conversion.
- Si/Al ratio 10 and wash treatment give highest ethanol-hydrogen conversion, 95.19%.
- Geothermal waste-derived catalyst was more suitable for framework/support catalyst.

ARTICLE INFO

ABSTRACT

The main aim of this work was to develop sustainable catalyst from geothermal waste by hydrothermal process for enhanced biohydrogen production. The effects of Si/Al ratio and pH neutralization on the catalyst were also investigated to provide further insight into the hydrogen production capability. Results have shown with increasing Si/Al ratio, a lower amount of catalyst was synthesized and smaller particle size was obtained. pH neutralization treatment resulted in higher conversion compared to non-neutralized ones. Meanwhile, the highest conversion of biohydrogen from ethanol through steam reforming process (95.19%) was obtained from catalyst with pH neutralization treatment and Si/Al ratio of 10. The catalyst developed in this study was concluded to be suitable for framework/supporting catalyst due to relatively low selectivity.

1. Introduction

Energy production systems of developed and developing countries rely heavily on fossil fuels. Despite the well-known consequences of prolonged fossil fuel uses, namely air pollution and global warming (Martins et al., 2018), this non-renewable source remained to be the preferred choice. Furthermore, the high demand for fuel and depleting resources of crude oil also adds to an unsustainable energy system (Day and Day, 2017) which elicit interest in alternative renewable energy to provide sustainable energy systems.

Lately, hydrogen is considered to be a viable alternative source of energy generator. Hydrogen generated energy only emits water as its side product, in other words, it emits zero greenhouse emission and counteracts the negative effects of fossil fuel usage (Banu et al., 2020; Preethi et al., 2019). Biohydrogen production can be achieved through various process technologies, including thermal pathways. This pathway known as steam reforming process requires the use of catalyst, typically nickel, platinum or rhodium (Efstathiou and Kalamaras, 2013). However, due to the relatively

expensive metals and limitation of metal resources for sustainability, an alternative catalyst is needed.

Zeolite recently emerged as a potential catalyst in industrial applications due to its high surface area, high adsorption capacity, and good molecular dimensions of the pores (Chica et al., 2012). Zeolite is microporous crystalline aluminosilicates, which can be derived from geothermal waste which is rich in silica. Geothermal waste is abundant, while its utilization currently is limited to fertilizer and cement raw material. Previous studies regarding the use of zeolite in steam reforming process have been conducted, Campos-Skrobot et al. (2008) studied the use of zeolite as support, stating that Na Y zeolite-supported Rh was a promising catalyst for ethanol steam reforming. Chica et al. (2012) conducted a study of Ni and Co supported on delaminated silica, reported that excellent catalytic performance was exhibited due to the low concentration of acid site in the zeolite, which inhibits the coke deposition thus slowing down the deactivation effects. This claim was further supported by research conducted by Inokawa et al. (2011) which reported that the catalytic performance was improved with increasing basic sites, where nickel supported zeolite resulted in the highest H_2 production. This study aims to develop a potential catalyst from geothermal waste by hydrothermal process for enhanced biohydrogen production and to assess the effect of SiO_2/Al_2O_3 (Si/Al) ratio and pH neutralization (wash treatment) on catalyst performance.

2. Materials and methods

2.1. Characterization of geothermal waste

Geothermal waste in the form of rocks obtained from geothermal power plant PT. Geo Dipa Energi located in Dieng, Wonosobo, Indonesia is characterized using Scanning Electron Microscopy - Energy Dispersive X-ray (SEM-EDX) analysis to determine its composition.

2.2. Variable and control

In this study, the control variables were geothermal waste size (125 μm) and mass (50 g), hydrothermal process at 150 °C for 5 h, steam reforming process operation time and temperature of 20 min and 300 °C, and 2 g of catalyst fed to the reactor on steam reforming process. The response variables were the yield of the catalyst and biohydrogen produced, the particle size of catalyst and the composition of biohydrogen. Whereas, the independent variables were the pH neutralizing treatment (washed and non-washed) and Si/Al ratio (2.5; 5; 7.5; 10; 12.5; 15).

The Si/Al ratio was applied to the reactor in the form of Al(OH)$_3$ addition on the catalyst synthesis. Al(OH)$_3$ was used as a source of alumina to form zeolite. Calculations based on moles of Si, Al, SiO$_2$, and Al$_2$O$_3$ were carried out to determine the amount of Al(OH)$_3$ added for each ratio variable.

2.3. Synthesis of catalyst

Geothermal waste rocks underwent pre-treatment procedure before it was synthesized as a catalyst. The pre-treatment started with the washing of the waste with demineralized water and drying. To reduce the size of the rocks, the waste was powdered with pestle and mortar and sieved to 125 μm. Geothermal waste in form of powder was calcined using tube furnace (Lindberg/Blue M, Asheville NC, USA) at 1000 °C with flowing air.

To synthesize the catalyst, 400 ml of 3 M NaOH (99%, Merck, Germany) was heated and stirred on 200 rpm, added with Al(OH)$_3$ (99.63%, Merck, Germany) until the solution was boiling and

Table 1
Geothermal waste composition.

Component	%w
Al_2O_3	0.05
Na_2O	0.19
SiO_2	35.09

transparent. 50 g of pre-treated geothermal waste was added and stirred on room temperature (25 °C) for 2 h. The solution undergoes hydrothermal process at 150 °C for 5 h to achieve crystallization. The temperature and time were chosen as it were the most common and optimum conditions to yield good properties of catalyst, such as high Si content, surface area, pore volume and crystallinity (Marler, 2019; Widayat et al., 2019; Vongvoradit; Worathanakul, 2012). To achieve a neutral pH, the catalyst was washed using demineralized water. The final step was eliminating impurities and carbon by calcination using tube furnace (Lindberg/Blue M, Asheville NC, USA) at 550 °C for 3 h with nitrogen flow. The yield of the catalyst was obtained by weighing the product formed after calcination using an electronic mass balance.

2.4. Catalyst characterization

The catalyst synthesized was analyzed using Particle Size Analyzer (PSA) to determine its particle size along with its size distribution. While the crystallinity of the catalyst was also investigated using X-ray Diffraction (XRD) method by observing the peak results. To analyze the surface morphology of the catalyst, SEM analysis was carried out. X-ray Fluorescence (XRF) analysis was carried out to further detect the heavy metals present on the catalyst.

2.5. Performance test

The steam reforming process conducted at 300 °C using the synthesized catalyst to produce biohydrogen was carried out as the performance test. 500 ml of ethanol (99.9%, Merck, Germany) mixed with demineralized water in a 1:9 ratio was fed into the evaporator. The vapor formed was pushed to the reactor by nitrogen gas. In the reactor, 2 g of catalyst was fed and as reaction took place, steam was produced and later condensed. Steam formed was tested with Gas Chromatography-Mass Spectrometry (GCMS) on the 12th min (the highest conversion). Meanwhile, steam formed was also condensed and tested with High-Performance Liquid
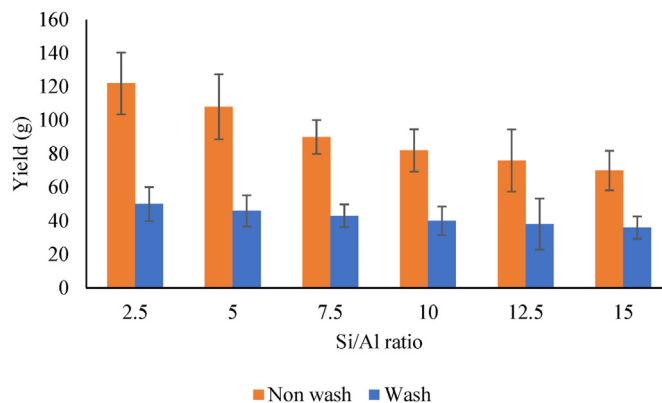

Fig. 1. Yield of catalyst.

Table 2
ANOVA analysis of wash and non-wash treatment on the synthesized catalyst's yield.

Source of Variation	SS	df	MS	F	P-value	F crit.
Si/Al ratio	15,857.5	5	3171.5	16.778	3.062E-12	2.298
Wash and non-wash treatment	72,520.8	1	72,520.8	383.657	2.467E-37	3.929
Interaction	5484.16	5	1096.83	5.803	8.7434E-05	2.298
Within	20,414.7	108	189.025			
Total	114,277	119				

Chromatography (HPLC). Biohydrogen conversion was then calculated using both analysis results.

3. Results and discussion

3.1. Components in geothermal waste

SEM-EDX analysis results of the geothermal waste composition were shown in Table 1. SiO_2 or silica was shown to be the highest component in the geothermal waste, 35.09%.

The presence of SiO_2 and Al_2O_3 were 2 main factors on the feasibility of geothermal waste being used as a raw material for zeolite synthesis. From the results of the analysis, geothermal waste was potential for zeolite synthesis due to its rich silica composition. The source of silica can affect numerous zeolite crystallization aspects, including but not limited to crystal growth kinetics and characteristics of final products. Also, different sources of silica used will significantly affect the results of zeolite synthesis (Yusof et al., 2010). Using rice husk ash as silica source would yield zeolite Y and ZSM-5 (Tolentino et al., 2020; Wang et al., 2019). While silica derived from fly ash would yield zeolite X and zeolite 4 A (Czuma et al., 2020; Iqbal et al., 2019).

3.2. Yield and characteristics of catalyst

In this study, synthesizing zeolite from geothermal waste with different variables affected the yield and characteristics of the catalyst. As shown in Fig. 1, the yield of catalyst varies on different ratios and treatments.

Washing treatment resulted in lower catalyst yield compared to non-wash treatment. According to the two-way ANOVA analysis with replication, the Si/Al ratio as well as wash and non-wash treatment was significant to the catalyst yield − proven by the obtained p value 3.06E-12 and 2.467E-37 respectively, which was less than $p = 0.5$ (Table 2). The purpose of washing treatment was to neutralize the basic pH of the catalyst solution, consequently reducing NaOH content on the solution. NaOH was responsible for the formation of zeolite crystals, indicated by research conducted by Fukui et al. (2006) which stated with higher NaOH concentration, the generation of zeolite crystals would be greater. This statement was also further backed-up by Yao et al. (2018) which stated that high alkaline concentration in the system will shorten the induction period and nucleation time, thus speeding up the rate of crystallization. Moreover, the increasing ratio of Si/Al also resulted in lower catalyst yield due to less $Al(OH)_3$ added. $Al(OH)_3$ acts as the source of aluminum due to the low percentage of
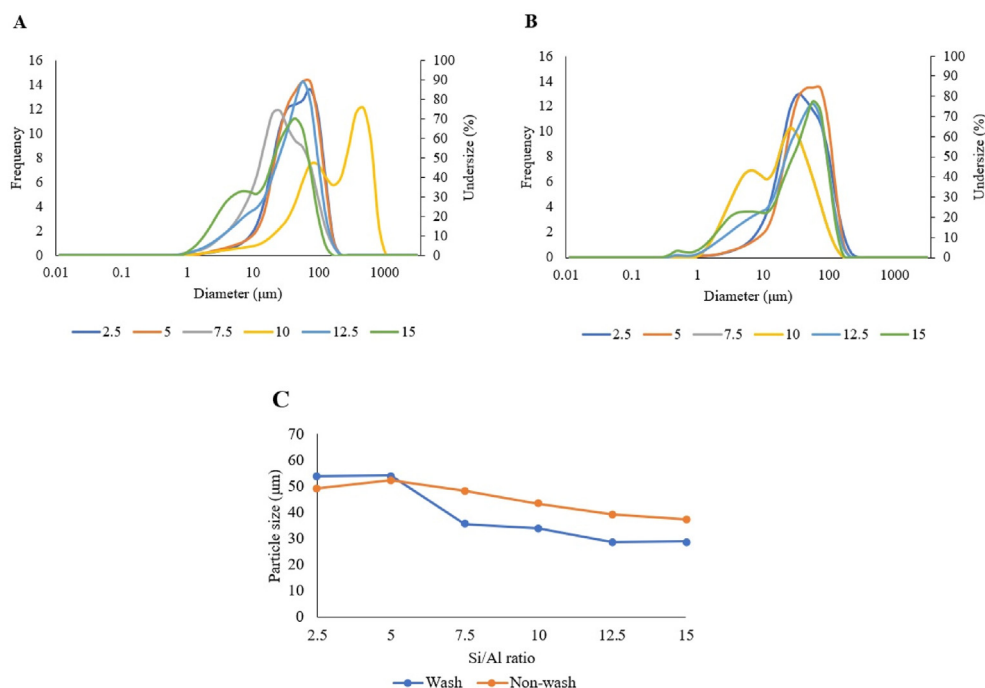

Fig. 2. Distribution of catalyst particle size (A) wash treatment (B) non-wash treatment and (C) relationship of Si/Al ratio to catalyst particle size.

Table 3
Heavy metals present in catalyst.

Element	Si/Al ratio							
	2.5		5		7.5		10	
	Wash	Non-wash	Wash	Non- wash	Wash	Non-wash	Wash	Non-wash
Al	2.931	2.231	2.587	2.166	2.522	2.3	2.817	2.613
Si	8.322	5.353	8.335	7.06	8.566	8.068	10.43	9410
P	4.476	3.764	4.085	3.839	3.819	3.88	4.473	4.445
S	5.657	4.882	5.07	4.808	4.727	4.839	5.448	5.235
Cl	7.755	6.722	6.806	6.574	6.322	6.549	7.267	7.653
K	20.758	18.167	19.189	18.317	18.5	18.095	21.496	21.496
Ca	11.509	9.674	10.381	10.239	9.775	9.967	12.356	11.356
Sc	7.034	6.11	5.97	5.828	5.666	5.854	6.706	6.726
Fe	–	1.33	2.598	2.368	2.88	2.78	6.955	6.951
As	3.095	8.215	5.589	6.334	7.561	7.226	1.362	1.362
Zr	–	1.482	1.659	1.638	1.555	1.619	2.14	2.041
Mo	3.281	2.961	2.811	3.005	2.441	2.753	2.625	2.665
Sb	2.407	2.041	2.209	2.667	1.409	1.689	2.053	2.051
Ba	2.113	1.879	1.968	2.248	1.512	1.741	1.672	1.572
Pb	3.348	8.9	6.049	6.836	8.15	7.793	1.485	1.473
Bi	–	3.4	2.331	2.679	3.1	2.988	0.563	0.533

| Element	Si/Al ratio			
	12.5		15	
	Wash	Non-wash	Wash	Non-wash
Al	1.963	1.323	2.411	1.295
Si	7.514	5.383	8.595	5.287
P	3.161	3.653	3.564	3.785
S	3.788	4.641	4.212	5.084
Cl	5.020	6.162	5.768	6.647
K	14.649	16.188	17.364	17.002
Ca	8.166	8.84	9.708	9.474
Sc	4.621	5.041	5.248	5.531
Fe	3.562	2.04	4.874	1.683
As	12.18	9.722	7.966	9.047
Zr	1.36	1.458	1.628	1.484
Mo	1.842	2.725	2.095	2.812
Sb	1.453	2.738	1.741	3.754
Ba	1.160	1.999	1.349	2.816
Pb	13.132	10.494	8.600	9.785
Bi	4.925	3.996	3.261	3.664
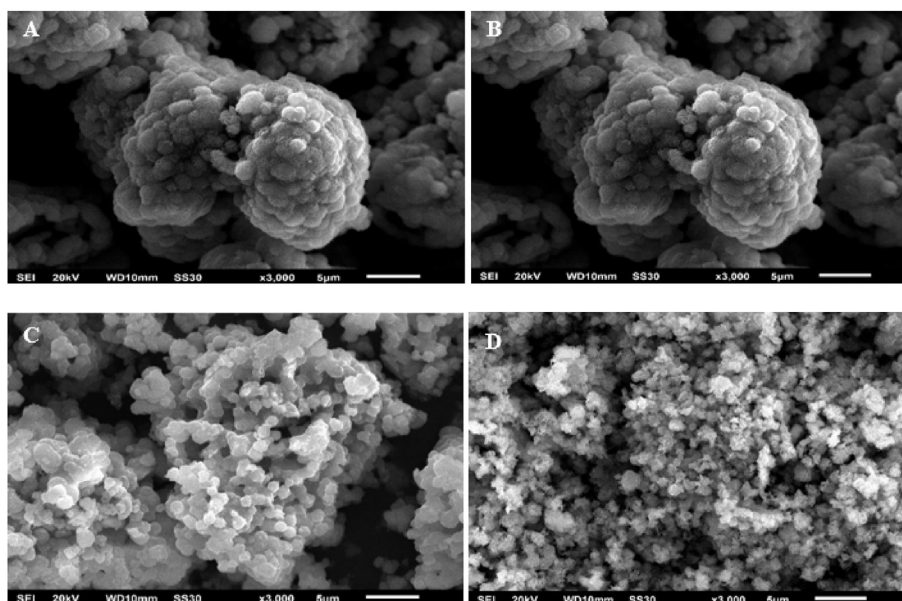
Fig. 3. Surface morphology of catalyst with was treatment and Si/Al ratio of (A) 2.5, (B) 5, (C) 12.5 and (D) 15.

aluminum in the geothermal waste (Table 1). The framework of zeolite consisted of networks of silica and aluminum. Therefore, decreasing the availability of aluminum in the precursor materials will inhibit the formation of zeolite crystals. This theory supported the ANOVA analysis results which concluded that the Si/Al ratio was dependent to the wash and non-wash treatment on the catalyst formation, as evidenced by the p value obtained, 8.74E-05 (Table 2).

Particle size and its distribution of the catalyst as shown in Fig. 2(A) and (B) for catalyst with washing treatment and non-washing treatment respectively was tested using PSA analysis. The particle diameters mainly fell in the micro size region (10−100 μm), although based on the wide distribution it could be drawn to a conclusion that the sizes were not homogenous. The catalyst particles were micro-sized due to the presence of water in the PSA analysis dispersion media agglomerating the particles and the presence of heavy metals as shown on the XRF analysis results (Table 3). Based on the XRF analysis, the presence of heavy metals was relatively high. Heavy metals would stick on the surface of the catalyst making it bulkier, hence contributing to a bigger size of the particle. Additionally, the slow increase of Si/Al ratio on the catalysts were to maintain the type of catalyst formed, which was faujasite zeolite (zeolite Y). Zeolite Y has a Si/Al ratio of 2−6 and is widely used as catalysts (Sadeghbeigi, 2012). Verboekend et al. (2016) supported this statement and further stated that Si/Al ratio greater than 6 would form ultra-stable Y zeolite (USY), which has high thermal stability − one of the properties that contributed to great catalytic activity.

In addition, based on the particle size distribution results, the average particle size was calculated towards its distribution (Fig. 2 (C)). Greater Si/Al ratio led to a smaller particle size on both wash and non-wash treatment. However, the catalyst with non-wash treatment has a bigger particle size compared to the wash treatment. Smaller size in the wash treatment catalyst was caused by particles leaching away during the washing process, thus reducing the chance of agglomeration. The calculation was supported by the SEM analysis of the catalyst with wash treatment which showed the surface morphology. Fig. 3(A) and (B) showed images of the catalyst particle with a Si/Al ratio of 2.5 and 5 respectively. It could be seen that both had more compact and bigger particle sizes compared to the catalyst with a higher Si/Al ratio of 12.5 and 15 (Fig. 3 (C) and (D), respectively). Moreover, the similarity on particle morphology of Si/Al ratio 2.5 and 5 were further supported by the insignificant particle size difference calculated in Figs. 3, 54.058 and 54.110 μm respectively.

The crystallinity of the catalyst synthesized was also investigated using the XRD analysis. Fig. 4(A) and (B) showed the results of the analysis for wash treatment and non-wash treatment respectively. The synthesized catalyst with wash treatment was concluded to have a crystalline structure based on the presence of many peaks in the result (Fig. 4 (A)). The highest peaks on Si/Al ratio of 2.5; 5; 7.5; 10; 12.5 and 15 were $2\theta = 34.650°$; $29.870°$; $29.743°$; $24.288°$; $27.330°$ and $29.781°$ respectively. Whereas in non-wash treatment results (Fig. 4 (B)), it could be seen that the peaks present were sharper compared to the wash-treatment − this indicates that the catalyst synthesized has higher crystallinity. The highest peaks on Si/Al ratio of 2.5; 5; 7.5; 10; 12.5 and 15 were $34.830°$; $29.890°$; $29.743°$; $24.288°$; $37.570°$ and $37.575°$ respectively. Nepheline $(Na,K)AlSiO_4$ was identified in every variable, except for Si/Al ratio 2.5 in the wash and non-wash treatment − which was identified as $Co_4Na_4Si_{12}Al_{12}O_{48}(NO)_3$ and sodium aluminum silicate respectively. Geothermal waste used in this study has Al_2O_3, Na_2O and SiO_2 components (Table 1) which when reacted with $Al(OH)_3$ and NaOH will form the zeolite catalyst (2.3). Sodium aluminum silicate $(Na_{12}AlSiO_5)$ produced in this study was a type of
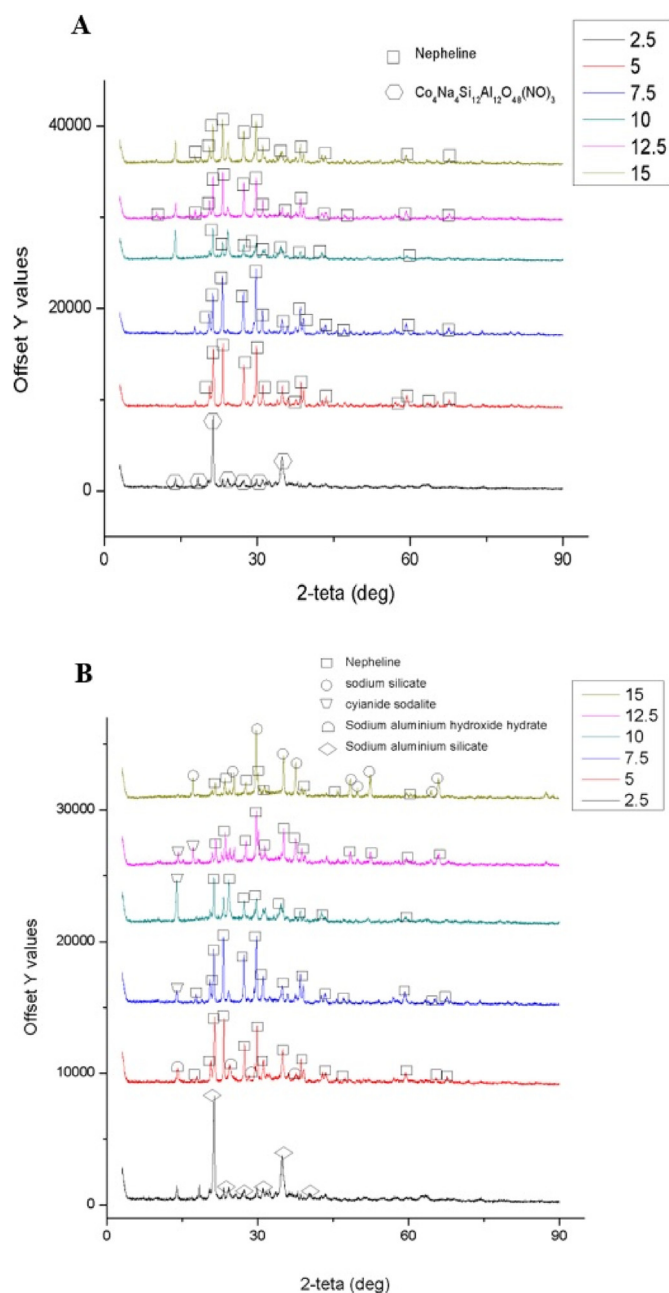

Fig. 4. Diffractogram of catalyst with (A) wash treatment and (B) non-wash treatment.

zeolite, which indicated that the catalyst synthesis was successful in Si/Al ratio 2.5 non-wash treatment. This conclusion was also further supported by the result of catalyst yield, in which Si/Al ratio 2.5 non-wash treatment has the highest catalyst yield (Fig. 1). Nepheline which was identified in almost all of the catalysts has a similar structure to zeolite, and its formation was due to insufficient addition of $Al(OH)_3$ (Hosseini, 2015). The presence of potassium in nepheline was also supported by the result in XRF analysis (Table 3). In conclusion, the wash and non-wash treatment, as well as Si/Al ratio have no significant effect on the crystallinity of the catalyst due to the fact that all catalyst has high crystallinity and almost uniform pattern (nepheline).
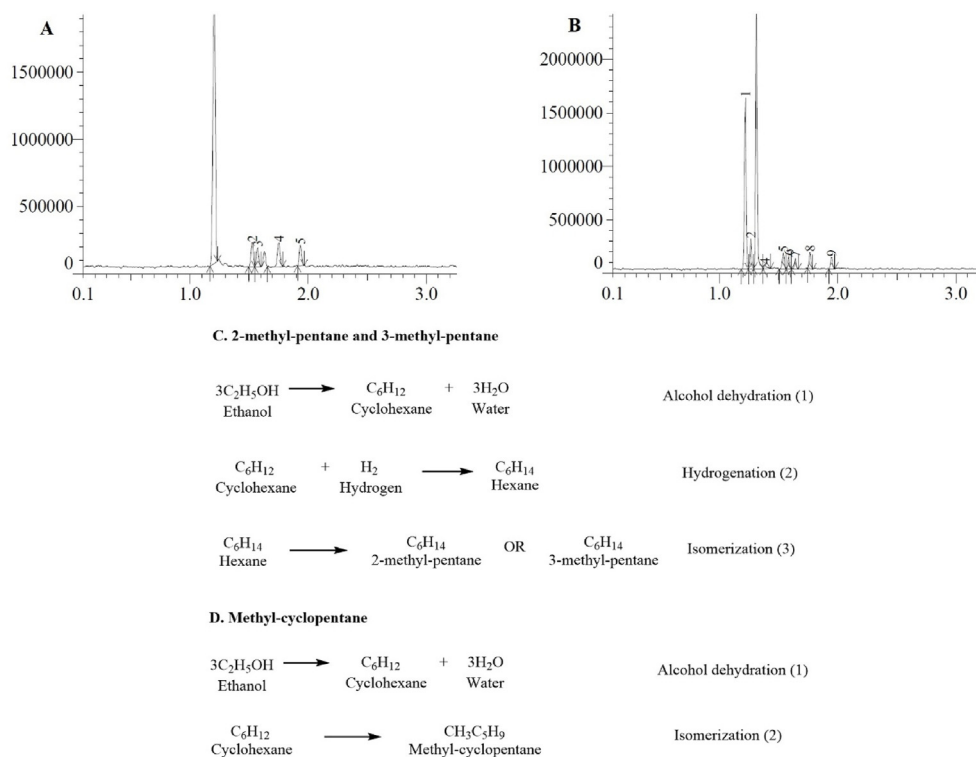
Fig. 5. GCMS result of biohydrogen with (A) washed, Si/Al ratio 10, and (B) non-washed Si/Al ratio 5, (C) 2-methyl-pentane and 3-methyl-pentane formation, (D) methyl-cyclopentane formation.

3.3. Yield and characteristics of biohydrogen produced

In the steam reforming process to produce biohydrogen, ethanol, and water as feed was converted to vapor and formed CO, H_2, CO_2, O_2 gases and hydrocarbon. GCMS analysis was used to determine the hydrocarbon components present in the product. GCMS results of biohydrogen with wash treatment and Si/Al ratio of 10 showed 2-methyl-pentane, 3-methyl-pentane, and methyl-cyclopentane as the highest peaks (Fig. 5 (A)). While for non-wash treatment with Si/Al ratio 5, the highest peaks shown were the same 2-methyl-pentane, 3-methyl-pentane, methyl-cyclopentane components, however with the addition of acetaldehyde (Fig. 5 (B)). The concentration of each component was also calculated, it was found that for Si/Al ratio 10 wash and 5 non-wash, 2-methyl-pentane yield 35.334% and 22.409% respectively; 3-methyl-pentane yield 25.749% and 14.800% respectively; methyl-cyclopentane yield 38.917% and 20.750% respectively, and acetaldehyde for Si/Al ratio 5 wash treatment yield 42.041%. Based on the results, the wash catalyst treatment and higher Si/Al ratio yield higher hydrocarbon concentration compared to the non-wash treatment with a lower Si/Al ratio. Fig. 5(C) and (D) showed the chemical reaction steps that took place on the formation of compounds identified by the GCMS analysis.

The basic equation used to describe the steam reforming process was:

$$C_2H_5OH + H_2O \rightarrow CO + H_2 + CO_2 + O_2 + C_xH_y \qquad (1)$$
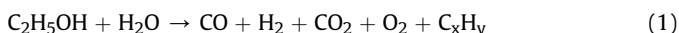
where C_xH_y was the hydrocarbon determined from the GCMS results.

HPLC analysis was also conducted to determine the ethanol residue on the gas produced from the steam reforming process. Along with the GCMS results of each variable, HPLC results of each variable of condensed gas were used in the calculation to determine the conversion of biohydrogen gas (H_2). Biohydrogen converted was calculated with the following equation:

$$Conversion(\%) = \frac{ethanol\,used - ethanol\,residue\,from\,HPLC\,results}{purity\,of\,ethanol\,used\,in\,the\,study}$$

$$(2)$$

From Fig. 6 (A), the conversion of biohydrogen with wash treatment for all Si/Al ratio was higher compared to conversion with non-wash treatment. Based on the ANOVA analysis, the Si/Al ratio was significant to the biohydrogen conversion, as indicated by the p-value obtained, 0.00671 (Table 4 (A)). Moreover, the wash and non-wash treatment were also significant with p-value 6.4E-07 (Table 4 (A)). The highest conversion was achieved by Si/Al ratio 10, 95.19%. This finding was supported by the results of the GCMS analysis (Fig. 5 (A)) which showed a higher concentration of hydrocarbon present in Si/Al ratio 10 with wash treatment. However, the conversion of biohydrogen without the use of catalysts was similar to the ones produced with catalysts. The ANOVA analysis results (Table 4 (B)) indicated that the synthesized catalyst has no significant difference to the biohydrogen conversion resulted with no catalyst usage (p = 0.62278). In other words, based on the biohydrogen conversion, the use of the synthesized catalyst in the steam reforming process was insignificant. In conclusion, the synthesized catalyst was more suitable as a framework/support catalyst, which should be impregnated with metals to increase its catalytic activity.
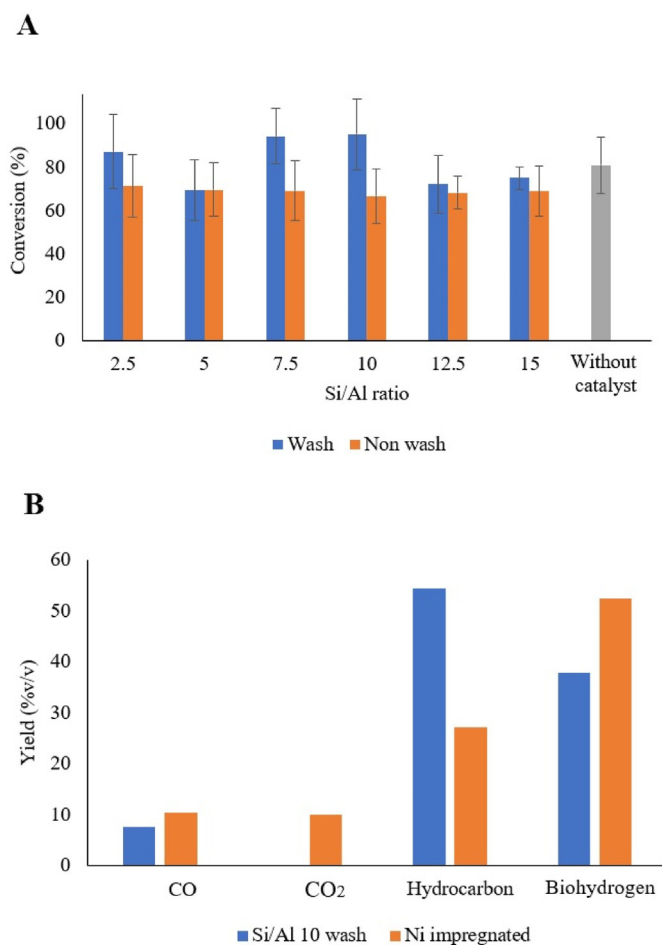
A

B

Fig. 6. Biohydrogen conversion to the study's variable (A) and yield between synthesized catalyst and Ni impregnated catalyst (B).

To confirm the conclusion, the synthesized catalyst was impregnated with nickel (the most commonly used metal in steam reforming process) and ethanol steam reforming process was carried out to compare the biohydrogen yield of the impregnated catalyst and the synthesized catalyst. Si/Al ratio 10 with wash treatment catalyst was chosen as the comparison variable as this catalyst gave the highest biohydrogen conversion. It was found that the Ni impregnated catalyst resulted in a higher biohydrogen yield

(52.356% v/v) compared to the Si/Al 10 with wash treatment catalyst, which only gave 37.917% v/v yield (Fig. 6 (B)). The high hydrocarbon content in the Si/Al 10 with wash treatment catalyst was due to the fact that this catalyst was more selective to hydrocarbon formation instead of biohydrogen formation. This statement could be explained by the hydrogenation reaction which took place in the steam reforming process (Kumar et al., 2014), where the formed hydrogen continued to react with ethanol to form hydrocarbon and water instead of stopping when hydrogen was formed. This was further supported by the low CO and no CO_2 content in the Si/Al 10 with wash treatment catalyst results, which has proven there was less hydrogen formed, as hydrogen was generally formed along with CO and CO_2 on the steam reforming and water gas shift reactions in the steam reforming process. To simplify, CO and CO_2 formed were directly proportional to H_2 formed (Kumar et al., 2014). Hence, low CO and CO_2 formed could be attributed to the fact that the synthesized catalyst was not selective to the steam reforming and water gas shift reaction which formed the hydrogen, instead directing the reaction path to the hydrogenation reaction which formed the hydrocarbons — which was supported by the high hydrocarbon concentration on the GCMS results (Fig. 5 (A)). Therefore, the conclusion that the Si/Al 10 with wash treatment catalyst was more suitable to be a framework catalyst was justified, as evidenced by its higher hydrocarbon and lower CO, CO_2 and hydrogen yield compared to when it was used as a support catalyst.

4. Conclusion

Geothermal waste is a potential raw material for catalyst in biohydrogen production. The washing treatment and increasing Si/Al ratio resulted in smaller catalyst particle size and lower catalyst yield. Based on the ANOVA analysis, Si/Al ratio and wash treatment were significant towards the catalyst yield and biohydrogen conversion. However, the use of catalyst on the biohydrogen production was insignificant due to the fact that the synthesized catalyst was more suitable as a framework/support catalyst. This statement was justified by the performance test results showing higher biohydrogen yield in nickel impregnated catalyst compared to the synthesized catalyst, which also has proven that the synthesized catalyst was not selective for biohydrogen formation.

Declaration of competing interest

The authors declare that they have no known competing financial interests or personal relationships that could have appeared to influence the work reported in this paper.

Table 4
ANOVA analysis on biohydrogen conversion for (A) wash and non-wash treatment, (B) wash treatment and without catalyst.

Source of Variation	SS	df	MS	F	P-value	F crit
A						
Si/Al ratio	3187.24	5	637.449	3.41033	0.00671	2.29843
Wash and non-wash treatment	5233.8	1	5233.8	28.0007	6.4E-07	3.92901
Interaction	3502.49	5	700.498	3.74764	0.00362	2.29843
Within	20,187	108	186.917			
Total	32,110.6	119				
B						
Si/Al ratio	3286.44	5	657.288	3.32345	0.00786	2.29843
Wash treatment and without catalyst	48.1334	1	48.1334	0.24338	0.62278	3.92901
Interaction	3286.44	5	657.288	3.32345	0.00786	2.29843
Within	21,359.5	108	197.773			
Total	27,980.5	119				

CRediT authorship contribution statement

Siti Munfarida: Investigation, Writing - original draft. **Widayat:** Conceptualization, Supervision, Project administration, Funding acquisition. **Hantoro Satriadi:** Methodology, Resources. **Bambang Cahyono:** Validation, Resources. **Hadiyanto:** Conceptualization, Data curation, Visualization. **John Philia:** Investigation, Formal analysis. **Jedy Prameswari:** Formal analysis, Writing - review & editing.

Acknowledgment

References

Banu, J.R., Kavitha, S., Kannah, R.Y., Bhosale, R.R., Kumar, G., 2020. Industrial wastewater to biohydrogen: possibilities towards successful biorefinery route. Bioresour. Technol. 298, 122378. https://doi.org/10.1016/j.biortech.2019.122378.

Campos-Skrobot, F.C., Rizzo-Domingues, R.C.P., Fernandes-Machado, N.R.C., Cantao, M.P., 2008. Novel zeolite-supported rhodium catalysts for ethanol steam reforming. J. Power Sources 183, 713−716. https://doi.org/10.1016/j.jpowsour.2008.05.066.

Chica, A., da Costa Serra, J.F., Navarro, M.T., Rey, F., 2012. Bioethanol steam reforming on Ni-based modified mordenite. Int. J. Hydrogen Energy 37, 7101−7108. https://doi.org/10.1016/j.ijhydene.2011.10.086.

Czuma, N., Zarebska, K., Motak, M., Galvez, M.E., Da Costa, P., 2020. Ni/zeolite X derived from fly ash as catalysts for CO_2 methanation. Fuel 267, 117139. https://doi.org/10.1016/j.fuel.2020.117139.

Day, C., Day, G., 2017. Climate change, fossil fuel prices, and depletion: the rationale for a falling export tax. Econ. Modell. 63, 153−160. https://doi.org/10.1016/j.econmod.2017.01.006.

Efstathiou, A.M., Kalamaras, C.M., 2013. Hydrogen production technologies: current state and future developments. Conference Papers in Energy 690627. https://doi.org/10.1155/2013/690627.

Fukui, K., Nishimoto, T., Takiguchi, M., Yoshida, H., 2006. Effect of NaOH concentration on zeolite synthesis from fly ash with a hydrothermal treatment method. KONA Powder Part. J. 24 https://doi.org/10.14356/kona.2006020.

Hosseini, S.A., 2015. Optimization of synthesis condition of zeolite 4A from nepheline syenite. Int. J. Mater. Chem. Phys. 1, 93−98.

Inokawa, H., Nishimoto, S., Kameshima, Y., Miyake, M., 2011. Promotion of H_2 production from ethanol steam reforming by zeolite basicity. Int. J. Hydrogen Energy 36, 15195−15202. https://doi.org/10.1016/j.ijhydene.2011.08.099.

Iqbal, A., Sattar, H., Haider, R., Munir, S., 2019. Synthesis and characterization of pure phase zeolite 4A from coal fly ash. J. Clean. Prod. 219, 258−267. https://doi.org/10.1016/j.jclepro.2019.02.066.

Kumar, A., Prasad, R., Sharma, Y.C., 2014. Steam reforming of ethanol: production of renewable hydrogen. Int. J. Environ. Res. 4, 203−212.

Marler, B., 2019. Hydrothermal synthesis of zeolites. Ruhr-universitat bochum. https://www.ruhr-uni-bochum.de/kristallographie/kc/mitarbeiter/marler/zeolites.html. (Accessed 5 April 2020).

Martins, F., Felgueiras, C., Smitkova, M., 2018. Fossil fuel energy consumption in European countries. Energy Procedia 153, 107−111. https://doi.org/10.1016/j.egypro.2018.10.050.

Preethi, Usman, T.M.M., Banu, J.R., Gunasekaran, M., Kumar, G., 2019. Biohydrogen production from industrial wastewater: an overview. Bioresour. Technol. 7, 100287. https://doi.org/10.1016/j.biteb.2019.100287.

Sadeghbeigi, R., 2012. Fluid Catalytic Cracking Handbook. Elsevier Inc. https://doi.org/10.1016/B978-0-12-386965-4.00004-5.

Tolentino, C.M.C., de Luna, M.D.G., Futalan, C.M., Choi, A.E.S., Manegdeg, F.G., Grisdanurak, N., 2020. Evaluation of the effect of hydrocarbons on hydrogen chloride removal from refinery off-gas using zeolite NaY derived from rice husks. Sci. Total Environ. https://doi.org/10.1016/j.scitotenv.2020.138782, 138782.

Verboekend, D., Nuttens, N., Locus, R., Aelst, J.V., Verolme, P., Groen, J.C., Perez-Ramirez, J., Sels, B.F., 2016. Synthesis, characterization and catalytic evaluation of hierarchical faujasite zeolites: milestones, challenges and future directions. Chem. Soc. Rev. 45, 3331−3352. https://doi.org/10.1039/C5CS00520E.

Vongvoradit, P., Worathanakul, P., 2012. Fast crystallization of SUZ-4 zeolite with hydrothermal synthesis: part I temperature and time effect. Procedia Eng 32, 198−204. https://doi:10.1016/j.proeng.2012.01.1257.

Wang, Y., Du, T., Fang, X., Jia, H., Qiu, Z., Song, Y., 2019. Synthesis of CO_2-adsorbing ZSM-5 zeolite from rice husk ash via the colloidal pretreatment method. Mater. Chem. Phys. 232, 284−293. https://doi.org/10.1016/j.matchemphys.2019.04.090.

Widayat, Hadiyanto, Satriadi, H., Cahyono, B., Astuti, W.I.S.T., Febrianti, P., 2019. Synthesis of zeolite x molecular sieve from geothermal solid waste. Mater. Today: SAVE Proc. 13, 137−142. https://doi.org/10.1016/j.matpr.2019.03.203.

Yao, G., Lei, J., Zhang, X., Sun, Z., Zheng, S., 2018. One-step hydrothermal synthesis of zeolite X powder from natural low-grade diatomite. Materials 11, 906. https://doi.org/10.3390/ma11060906.

Yusof, M.A., Nizam, N.A., Rashid, N.A.A., 2010. Hydrothermal conversion of rice husk ash to faujasite-types and NaA-type of zeolites. J. Porous Mater. 17, 39−47. https://doi.org/10.1007/s10934-009-9262-y.